Validation of Changes in Plasma miRNA Before and After Excision of Benign and Malignant Colorectal Neoplasia

Kayla Feagins AS[1], Jane Carter MB ChB[1], Uri Netz MD[1], M. Robert Eichenberger MS[1], Susan Galandiuk MD[1]

[1]Price Institute of Surgical Research and the Section of Colorectal Surgery, Hiram C. Polk Jr. MD Department of Surgery, University of Louisville School of Medicine, Louisville, KY

Introduction

- Colorectal cancer (CRC) is common worldwide and is the second leading cause of cancer death
- The best characterized pathway leading to the development of CRC is the adenoma-carcinoma sequence:
  Normal colon epithelium → Colorectal Advanced Adenomas (CAA) → Colorectal Adenocarcinoma
- microRNAs (miRNAs) are short, non-coding RNAs that play an important role in gene expression
- miRNAs have been associated with both the diagnosis and regulation of different disease processes
- They are closely associated with cell differentiation, proliferation, and apoptosis, all very important processes in tumorigenesis
- Current plasma-based assays used for monitoring response to therapy **lack sensitivity and specificity** for detecting recurrence of disease
- We believe miRNAs have a potential role in monitoring therapy following removal of a colorectal adenoma or cancer
- We have previously identified changes before and after excision of plasma miRNA expression in patients with CAA and CRC
- Our aim is to validate a panel of 11 significantly dysregulated miRNAs identified from screening of plasma samples from patients obtained before and after endoscopic or surgical removal of colorectal neoplasia

Hypothesis

- We hypothesize that miRNA expression differs between pre-treatment samples and post-removal samples of colorectal neoplasia

Methods

- Following informed consent, blood samples were taken from patients prior to and after removal of colorectal neoplasia
  - 12 patients with advanced CAA (>0.6 cm diameter +/or villous component)
  - 12 patients with stage II or III CRC
- Plasma was isolated from each patient sample (n=48)
- Total RNA was extracted from plasma (Qiagen® miRNeasy) and quality and quantity were assessed
- Reverse Transcription followed by quantitative real-time polymerase chain reaction (qRT-PCR) was performed using specific primers and probes to the 11 miRNAs of interest
- Data analyzed using paired t-tests after normalizing raw cycle threshold data to endogenous miR-16 and RNU6

Study Design

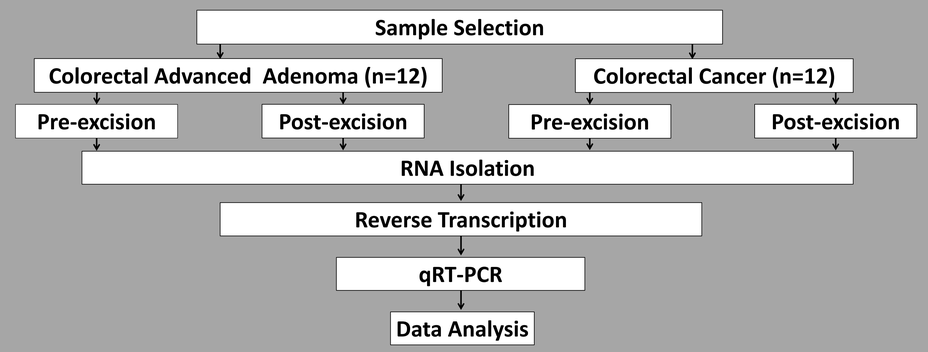

Results

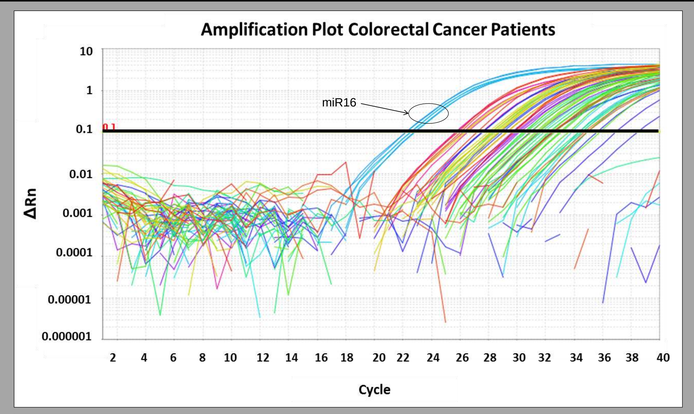

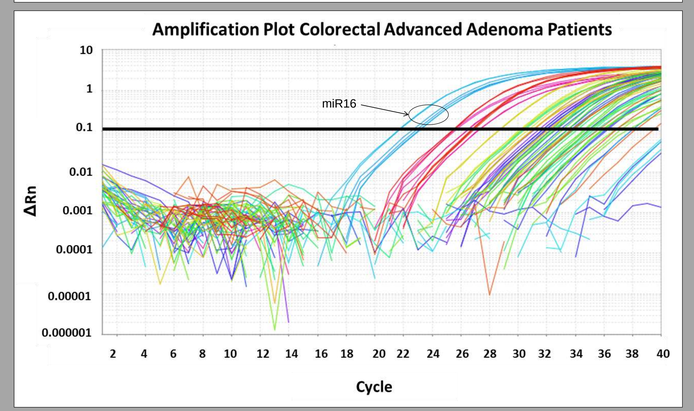

Results (cont.)

Colorectal Cancer

Target Name	ΔCT Pre	ΔCT Post	ΔΔCT	Fold Change	Fold Regulation	p-value
let7b	0.813	-1.051	1.864	1.039	1.039	0.061
miR19b	-2.097	-3.447	1.350	3.494	3.494	0.273
miR324-5p	4.615	2.594	2.022	0.670	-1.492	0.019
miR454	6.633	4.830	1.803	0.787	-1.270	0.043
miR29c	3.467	1.143	2.324	0.510	-1.962	0.027
miR122	-1.927	-3.905	1.979	0.845	-1.183	0.069
miR192	0.605	0.081	0.524	1.347	1.347	0.408
miR21	-0.553	-2.009	1.456	2.539	2.539	0.245
miR346	5.527	3.978	1.550	0.994	-1.006	0.058
miR372	5.210	3.372	1.838	0.858	-1.165	0.039
miR374a	3.809	1.655	2.154	0.726	-1.378	0.036
u6	Housekeeper					
miR16	Housekeeper					

Colorectal Advanced Adenoma

Target Name	ΔCT Pre	ΔCT Post	ΔΔCT	Fold Change	Fold Regulation	p-value
let7b	2.587	1.340	1.247	0.740	-1.351	0.079
miR19b	-1.889	-2.358	0.470	0.992	-1.008	0.362
miR324-5p	7.794	7.797	-0.003	2.335	2.335	0.997
miR454	5.941	5.051	0.891	0.936	-1.068	0.113
miR29c	4.037	3.799	0.239	1.288	1.288	0.604
miR122	5.356	3.917	1.439	1.359	1.359	0.075
miR192	3.701	3.355	0.346	1.487	1.487	0.594
miR21	-2.162	-2.566	0.405	0.941	-1.063	0.240
miR346	8.429	8.980	-0.551	4.274	4.274	0.460
miR372	9.791	9.778	0.013	4.794	4.794	0.987
miR374a	5.605	4.585	1.020	0.665	-1.505	0.016
u6	Housekeeper					
miR16	Housekeeper					

Conclusions and Future Directions

- We validated expression levels of 5 miRNAs (miR-324-5p, miR-454, miR-29c, miR-372 & miR-374a) to be different in pre-treatment compared to post-removal plasma samples in patients with CRC and CAA
- miR-374a was significantly downregulated in both CRC and CAA in pre-treatment samples compared to post-treatment samples
- These findings may help provide for a relatively non-invasive method of monitoring therapy or assessing response to treatment and can be used as an innovative tool in diagnostics
- Future considerations should include more specific miRNAs that play a role in initiation, progression, and outcomes in colorectal cancer and the use of miRNAs as potential therapeutic targets

Acknowledgments

National Cancer Institute grant R25-CA134283, John Williamson and Barbara Thruston Atwood Price Trust

Rest-activity Rhythms and Quality of Life in Lung Cancer Patients

Olivia Fields[1], Elizabeth Cash, PhD[1,2,3], Lauren A. Zimmaro, MA[1], Allison Hicks, BA[1], Christy Albert, BS[2], Sandra E. Sephton, PhD[1,2]

[1] Department of Psychological and Brain Sciences, University of Louisville, Louisville, KY. [2]J.G. Brown Cancer Center, University of Louisville, Louisville, KY.

[3]Department of Otolaryngology- HNS and Communicative Disorders, University of Louisville School of Medicine, Louisville, KY.

Learning Objective

This study aims to examine the relationship between rest-activity rhythms and quality of life in lung cancer patients as both are strong predictors in cancer survival and prognosis.

Abstract

BACKGROUND

Quality of life and rest-activity rhythms have been shown to be strong predictors of cancer prognosis and survival[3,5,8,9]. However, few studies have examined how these two predictors relate to each other. We investigate the association between quality of life and rest-activity rhythms.

METHODS

Lung cancer patients (N=49) filled out the FACT-L questionnaire to obtain overall and subscales of quality of life (QOL). Wrist-ware actigraphy watches were worn to collect rest-activity data. We examined autocorrelation (r24), nighttime restfulness (I<O) and daytime sedentariness (O<I) predicting quality of life. In hierarchical regressions controlling for gender, age at diagnosis, stage, and income, variables were entered in separate regressions examining 6 scores of QOL: health-related overall, physical, social-family, emotional, functional, and lung specific well-being.

RESULTS

Hierarchical regressions found significant relationships between I<O and physical well-being. Lung cancer patients with more nighttime restfulness had higher physical well-being (p= .016). Significant results were also present when controlling for age testing relationships between SFWB and r24 (p= .026), and SFWB and I<O (p= .028), indicating older lung cancer patients have higher SFWB scores.

CONCLUSIONS

This study supports past research in the integration of rest-activity rhythms and quality of life measures in diagnostics. It also shows a significant link between the two predictors.

RESEARCH IMPLICATIONS: Research should continue to investigate the relationship between rest-activity rhythms and quality of life. Possible explanations could be a third physiological variable such as endocrine or immune function.

CLINICAL IMPLICATIONS: Lung cancer patients experiencing rest-activity disruption should be screened for areas of quality of life. Future research should continue the notion of integrating quality of life and rest-activity rhythm measures in prognostic and survival diagnosis.

Background

Lung cancer is the second most common cancer in men and women. Distress from initial diagnosis and continued lung cancer treatments can lead to a decrease in quality of life (QOL). Numerous studies have shown quality of life to be a significant prognostic and survival predictor in lung cancer patients[8,9]. Quality of life is a multidimensional concept that includes subjective evaluations of positive and negative aspects of life. A reliable QOL survey pertaining to lung cancer patients is the Functional Assessment of Cancer Therapies- Lung Cancer (FACT-L),[7] which includes dimensions and subscales shown in Figure 1.

Circadian coordination has been shown to have strong tumor-suppressive actions in laboratory and animal studies[2]. In humans, circadian rhythms of rest versus activity cycles are prognostic for colorectal cancer survival and may predict response to treatment[3]. Circadian rhythms are a system composed of molecular clocks that synchronize physiological functions, such as the cell cycle and apoptosis, in a 24-hour cycle[10]. Rest-activity rhythms are also one of the many circadian rhythms in the body. There is evidence that disruption of circadian rhythms can lead to tumor promoting environments[2, 3].

There is a scarcity of research on the relationship between these two prognostic factors in lung cancer patients: rest-activity rhythms and quality of life. Therefore, this study aims to evaluate the relationship between these two variables among a sample of lung cancer patients.

Hypothesis

Lung cancer patients with more disrupt rest-activity rhythms will have lower quality of life and poorer scores on FACT-L.

Model Summary Overall

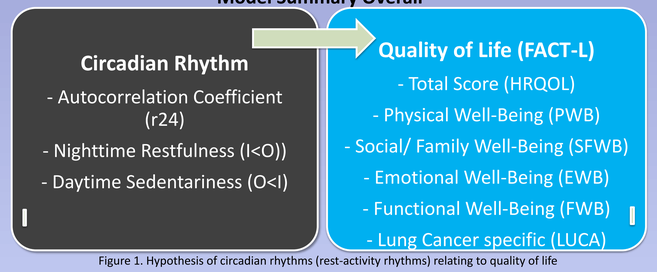

Figure 1. Hypothesis of circadian rhythms (rest-activity rhythms) relating to quality of life

Model Showing Predictors and Outcomes

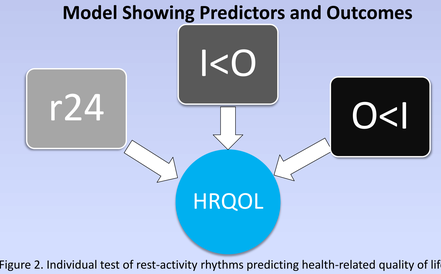

Figure 2. Individual test of rest-activity rhythms predicting health-related quality of life

Methods

PARTICIPANTS

Non-small cell lung cancer patients (N=49, 14 males, 35 females) diagnosed within the last 5 years provided demographics and self-report measures of quality of life (FACT-L). Participants wore an actigraphy watch for 10 consecutive days and filled out daily questionnaires giving time of wake and bed along with times the watch was removed.

MATERIALS

To calculate rest-activity rhythms ACTi graph Action4 software was used, and data were binned over time in bed (TIB) intervals. Intervals were marked based on the daily questionnaire times and visual inspection of the data. The software calculated autocorrelation coefficient (r24), a measure of regulation of daily activity calculated by taking a correlation of 1-minute epochs on one day with the same epoch on different days to give a 24-hour correlation; nighttime restfulness (I<O), the percent of time in bed in which activity falls below the median of activity out of bed (higher scores indicate more restfulness); and daytime sedentariness (O<I), the percent of time out of bed in which activity falls below the median of activity in bed (higher scores indicate more sedentary behavior).

The Functional Assessment of Cancer Therapy-Lung (FACT-L) is a 44-item self-report instrument, which measures multidimensional quality of life among lung cancer patients. Measures are listed in Figure 1.

STATISTICAL ANALYSIS

Prior to analysis, actigraphic data were were log transformed. Separate regressions were run using the independent and dependent variables for each pathway outlined in Figure 1, yielding a total of 18 regressions. In all hierarchical multiple regressions, control variables (gender, age of diagnosis, cancer stage, income) were entered in Model 1. In Model 2, independent were added to the overall models predicting overall health-related quality of life score, and the subscale scores.

Table 1. Patient Characteristics

Control Variables	Mean (SD) or Frequency		Predictor and Outcome Variables		Mean (SD)
Age at Cancer Diagnosis	59.57 years (9.35860)		Rest-activity Rhythms	R24	.1666 (.08)
Income (in thousands)	>$20	34.9%		I<O	93.26 (4.97)
	$20-39.9	27.9%		O<I	3.11 (5.26)
	$40-59.9	9.3%	FACT-L Total	HRQOL	90.70 (21.50)
	$60-79.9	11.6%	FACT-L subscales	PWB	20.24 (5.12)
	$80-99.9	4.6%		SFWB	18.07 (5.96)
	<$100	11.6%		EWB	17.23 (5.19)
Cancer Stage	Stage I	22.4%		FWB	17.21 (6.54)
	Stage II	10.2%			
	Stage III	38.8%		LUCA	17.96 (5.39)
	Stage IV	28.6%			

Image from Action4 Software of Rest-activity Rhythms

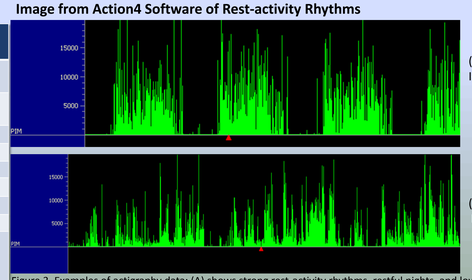

Figure 3. Examples of actigraphy data; (A) shows strong rest-activity rhythms, restful nights, and low sedentary behavior; (B) shows disrupted rest-activity rhythms, less restful nights and more sedentary

Lung cancer patients with more nighttime restfulness had higher physical well-being. Younger lung cancer patients had lower physical well-being. Younger lung cancer patients also had lower social and family well-being.

Regression analyses showing lung cancer patients with lower physical well-being have less nighttime restfulness. Younger lung cancer patients have higher physical well-being.						
	Model 1 (Control Variables)			Model 2 (Full Model)		
Variables	B	Std. Error	Beta	B	Std. Error	Beta
Age at Diagnosis	0.161	0.089	0.295	0.174	0.083	***0.318**
Stage (from Chart)	0.594	0.803	0.129	0.439	0.748	0.096
Gender	1.866	1.954	0.166	1.201	1.832	0.107
Income	1.495	1.074	0.232	0.838	1.029	0.13
I<O				-2.518	0.99	***-0.394**
R2		0.139			0.28	
F for change in R2		1.373			***6.471**	
Dependent Variable: PWB						
*p < .05						
I<O Inside Dichotomy Index, PWB Physical Well Being						

Table 2. Hierarchical regressions of I<O being a predictor of PWB with significant relationships marked with a *.

More Nighttime Restfulness Shows Higher Physical Well-Being

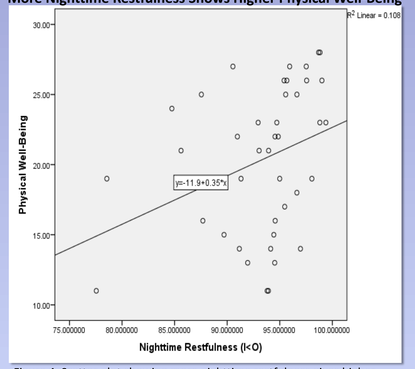

Figure 4. Scatter plot showing more nighttime restfulness gives higher physical well-being in lung cancer patients.

Results

Hierarchical regressions revealed significant relationships between nighttime restfulness and physical well-being (PWB). Lung cancer patients with more nighttime restfulness had higher PWB scores (p= .016). Age was also a significant predictor such that younger patients had poorer well being when I<O was the predictor and PWB was the outcome (p= .043). Significant results were also present when controlling for age testing relationships between r24 and social-family well-being (SFWB) (p= .026), and I<O and SFWB (p= .028), indicating older lung cancer patients have higher social-family well-being scores. No other significant relationships were found in this study.

Conclusions

- Nighttime restfulness and PWB, in addition to being related to cancer prognosis and survival rates in other cancers, are significantly related to each other in lung cancer patients.
- Poor physical well-being in younger patients may reflect more aggressive tumors, although stage was not associated with QOL, suggesting QOL gives different information than stage for prognostics and course of cancer treatment.
- Older lung cancer patients had higher social-family well-being. This could be due to more developed long-term relationships in older individuals, in general.
- Several other studies have suggested QOL and rest-activity rhythms provide useful information for cancer prognosis and survival[1,3,5,8,9]. Many have also suggested these two variables should be considered in cancer survival diagnosis in multiple cancers[1,3,5,8,9]. This study supports both these notions as understanding their relationship could give more information on their prognostic value and support their integration in diagnosis.
- Future research should continue to explore the relationship between rest-activity rhythms and quality of life.
- Further investigation of the association between rest-activity rhythms and QOL could reveal a third driving variable, such as endocrine or immune function[4].

Acknowledgements

Funding support was provided by National Cancer Institute grant R25-CA134283 and is gratefully acknowledged.

References

1. Eismann, E. A., Lush, E., & Sephton, S. E. (2010). Circadian effects in cancer-relevant psychoneuroendocrine and immune pathways. Psychoneuroendocrinology, 35(7), 963-976.
2. Fu, L., & Lee, C. C. (2003). The circadian clock: pacemaker and tumour suppressor. Nature Reviews Cancer, 3(5), 350-361.
3. Mormont, M. C., Waterhouse, J., Bleuzen, P., Giacchetti, S., Jami, A., Bogdan, A., ... & Lévi, F. (2000). Marked 24-h rest/activity rhythms are associated with better quality of life, better response, and longer survival in patients with metastatic colorectal cancer and good performance status. Clinical Cancer Research, 6(8), 3038-3045.
4. Cash, E., Sephton, S. E., Chagpar, A. B., Spiegel, D., Rebholz, W. N., Zimmaro, L. A., ... & Dhabhar, F. S. (2015). Circadian disruption and biomarkers of tumor progression in breast cancer patients awaiting surgery. Brain, behavior, and immunity, 48, 102-114.
5. Dedert, E., Lush, E., Chagpar, A., Dhabhar, F. S., Segerstrom, S. C., Spiegel, D., ... & Sephton, S. E. (2012). Stress, coping, and circadian disruption among women awaiting breast cancer surgery. Annals of behavioral medicine, 44(1), 10-20.
6. Casso, D., Buist, D. S., & Taplin, S. (2004). Quality of life of 5–10 year breast cancer survivors diagnosed between age 40 and 49. *Health and quality of life outcomes*, *2*(1), 1.
7. Cella, D. F., Bonomi, A. E., Lloyd, S. R., Tulsky, D. S., Kaplan, E., & Bonomi, P. (1995). Reliability and validity of the Functional Assessment of Cancer Therapy—Lung (FACT-L) quality of life instrument. Lung cancer, 12(3), 199-220.
8. Polanski, J., Jankowska-Polanska, B., Rosinczuk, J., Chabowski, M., & Szymanska-Chabowska, A. (2016). Quality of life of patients with lung cancer. OncoTargets and therapy, 9, 1023.
9. Braun, D. P., Gupta, D., & Staren, E. D. (2011). Quality of life assessment as a predictor of survival in non-small cell lung cancer. BMC cancer, 11(1), 1.
10. Rich, T., Innominato, P. F., Boerner, J., Mormont, M. C., Iacobelli, S., Baron, B., ... & Lévi, F. (2005). Elevated serum cytokines correlated with altered behavior, serum cortisol rhythm, and dampened 24-hour rest-activity patterns in patients with metastatic colorectal cancer. *Clinical Cancer Research*,*11*(5), 1757-1764.

Differential Regulation of lncRNAs by *Poryphoromonas gingivalis* in Oral Squamous Cell Carcinoma

Z. Fitzsimonds, M. Sztukowska, E. Rouchka, T. Kalbfleisch, D. Darling, M. Metzler and R. Lamont
Department of Oral Immunology and Infectious Disease, University of Louisville School of Dentistry

UNIVERSITY OF LOUISVILLE
It's Happening Here.

Abstract

Objective: To measure the expression of Long-non coding RNAs (lncRNAs) using qRT-PCR in TIGK cells infected with *Porphyromonas gingivalis*.

Background: Long-non coding RNAs are RNAs that are longer than 200bp, and lack protein coding potential. LncRNAs make up almost a third of the total RNAs found in the human genome as seen in Figure 1, but they have been the least studied. These RNAs have been implicated in several types of cancers, such as gastric, liver, and colon cancer. Little is known mechanistically how lncRNAs operate, however in several knockout experiments of Linc00152 the tissue showed decreased invasiveness and decreased cell proliferation. These RNAs can be the key to understanding tumor carcinogenesis, and also provide crucial biomarkers for cancers that have minimal diagnostic capability. Epithelial to Mesenchymal Transition (EMT) is a method by which epithelial tissue undergo a morphological change. This changes allows for epithelial cells to adopt an undifferentiated invasive phenotype, which disrupts the basement membrane allowing for invasion of the bloodstream. Telomerase immortalized gingival keratinocytes were designed in our lab from gingival epithelial cells, and have been shown when infected with PG to undergo EMT. There are limited biomarkers to identify oral squamous cell carcinoma and its progression, so investigating lncRNA expression may help identify novel biomarkers.

Methods: Telomerase immortalized gingival keratinocytes were grown to 60-80% confluence, and then infected with *P. gingivalis*. RNAseq data for non infected and *P. gingivalis* infected TIGK cells were aligned to human reference genome Hg37 using Tophat, and differential expression of lncRNAs between no infection (NI) and infected TIGK cells were analyzed using Cufflinks. P-values ≤ 0.05 were considered significant.

Results: linc00152 showed significant upregulation by *P. gingivalis* in infected TIGK cells compared to the control no infected TIGK cells.

Conclusions: The lncRNA investigated in this study was significantly regulated by *P. gingivalis*. *P. gingivalis* can induce epithelial to mesenchymal transition in TIGK cells, which is a biomarker for oral squamous cell carcinoma. The purpose of this regulation is not yet understood, but investigating the mechanism by which these lncRNAs operate within the cell will be useful in identifying oral squamous cell carcinoma in patients presenting with OSCC symptoms.

Introduction

48,250 Americans are diagnosed with Oral Cancer each year, and the survival rate at 5 years is approximately 57% according to the oral cancer foundation. Oral Squamous Cell Carcinoma appears asymptomatic at first, and has limited diagnostic biomarkers to identify the progression of the tumor. Epithelial to Mesenchymal Transition (EMT) markers are used to identify the cancer currently[1]. EMT is the process by which the normal epithelial tissue has undergone a morphological change, and adopts an invasive myofibroblast phenotype as seen in Figure 2[1]. The now mesenchymal cells can invade the basement membrane, enter the bloodstream, and then undergo Mesenchymal to Epithelial transition to aggregate and metastasize[1]. *P. gingivalis* is an oral gram negative pathogen that has been implicated in OSCC. One of the mechanisms by which EMT has been characterized in gingival epithelial cells is the upregulation of Zeb1/2, which are key transcriptional regulators in the transition to this invasive phenotype[2][3][4]. Long-non coding RNAs are RNAs longer than 200bp, and lack protein coding potential. Recent studies have implicated lncRNAs in increased invasiveness and cell proliferation in gastric, liver, and kidney cancers[5][6]. lncRNAs have not been investigated in OSCC, and have been shown to be significantly up/down regulated based on preliminary RNAseq statistical analysis of telomerase immortalized keratinocytes infected with *P. gingivalis*.

References

[1] Scanlon, C., Van Tubergen, E., Inglehard, R., and D'Silva, N. "Biomarkers of epithelial-mesenchymal transition in squamous cell carcinoma." *J Dent Res*. 2013 Feb;92(2):114-21.

[2] Yilmaz, O., Verbeke, P., Lamont, R., and Ojcius, D. "Intracellular spreading of *Porphyromonas gingivalis* infection in primary gingival epithelial cells." *Infect Immun.* 2006 Jan;74(1):703-10.

[3] Inaba, H., et al. *Porphyromonas gingivalis* promotes invasion of oral squamous cell carcinoma through induction of proMMP9 and its activation." *Cell Microbiol*. 2014 Jan; 16(1): 131-145.

[4] Sztukowska, M., et al. *Porphyromonas gingivalis* initiates a mesenchymal like transition through ZEB1 in gingival epithelial cells." *Cell Microbiol*. 2016 June; 18(6): 844-858.

[5] Deng, L, Yang, S., Xu, F. and Zhang, J. "Long noncoding RNA CCAT1 promotes hepatocellular carcinoma progression by function as a let-7 sponge." *J. Exp. Clin. Cencer Res.*; 2015 Feb; 34: 18.

[6] Zhao, J. et al. "Long non-coding RNA Linc00152 is involved in cell cycle arrest, apoptosis, epithelial to mesenchymal transition, cell migration, and invasion in gastric cancer." *Cell Cycle.* 2015 July; 14 (19): 3112-3123.

Background

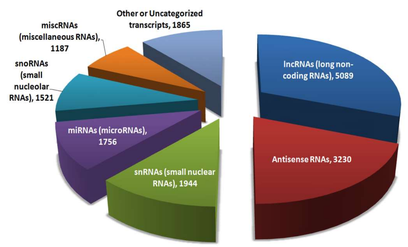

Figure 1: lncRNAs are RNAs that are >200bp long, and lack protein coding potential lncRNAs compose a majority of the total RNAs expressed in the human genome. Investigation of these RNAs has recently become popular, and now they have been shown to be differentially regulated in different types of cancers.

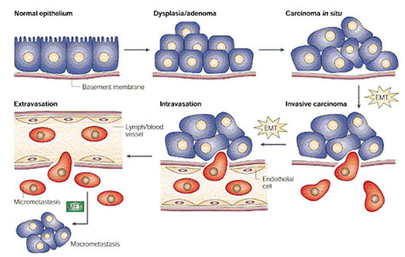

Figure 2: Epithelial to Mesenchymal Transition (EMT) is a key process in normal tissue adopting a cancerous phenotype. Epithelial tissue down regulate E-cadherin expression, which then allows the cells to break apart and disrupt the basement membrane. By use of matrix metalloproteinases the cells can invade the underlying tissues, and metastasize into the blood.

Methods

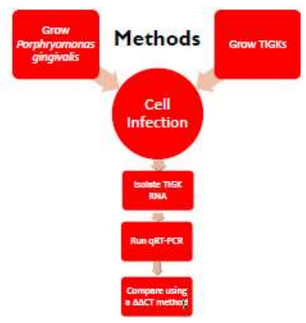

Primers were designed for each lncRNA of interest, and then tested for efficiency using RT-PCR. TIGK cells and *P. gingivalis* cells were grown, and then TIGK cells were challenged with *P. gingivalis* at MOI 50 and 100. Total RNA was extracted, reverse transcribed, and then lncRNA expression was analyzed using qRT-PCR. ΔΔCT values were analyzed using a two-way ANOVA test, and a P -value < .05 was considered significant.

Results

RNAseq for no infected TIGK cells, and TIGK cells infected with *P. gingivalis* were compared. Those lncRNAs with significant upregulation are shown in Table 1.

Transcript	NI TIGK Expression	PG Infected TIGK Expression	Fold Change
lnc-CD38-4:1	2.98178	25.5881	8.581501
lnc-HSPB7-2:1	7.22986	40.7811	5.640644
lnc-SMAD6-3:1	43.3165	221.686	5.117822
lnc-ZNF674-12:1	12.5662	61.4768	4.892256
Linc00152	5.48295	26.4322	4.820799
lnc-DEFB134-1:1	9.39624	40.8831	4.351009

Table 1: Upregulated lncRNAs

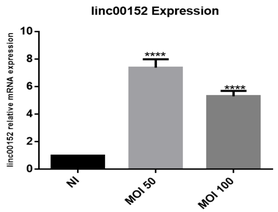

linc00152 expression was measured in no infected, multiplicity of infection (MOI) 50, and 100 using qRT-PCR. There is a significant upregulation of linc00152 in TIGK cells when *P. gingivalis* is present.

Those lncRNAs that are significantly downregulated in the presence of PG are shown in Table 2

Transcript	NI TIGK Expression	PG Infectected TIGK Expression	Fold Change
lnc-LEPREL1-8:1	161.441	18.1353	0.112334
lnc-RAD51-2:1	862.756	45.2292	0.052424
lnc-CDHR5-2:1	4100.31	150.114	0.03661
lnc-IFITM2-5:1	3432.12	67.1824	0.019575
lnc-PAPSS2-3:1	24827	455.361	0.018341

Table 2: Downregulated lncRNAs

Conclusions

- linc00152 is significantly upregulated by *P. gingivalis* in TIGK cells
- lncRNAs may play key regulatory role in Epithelial to Mesenchymal Transition
- Further investigation may lead to novel biomarkers for OSCC by lncRNA expression

Future Studies

- Measure expression of genes local to these lncRNAs to investigate whether lncRNAs differentially regulate them
- Knockout lncRNAs, and investigate the effect it has on EMT and invasiveness of TIGK cells

Acknowledgments

- National Cancer Institute grant R25-CA134283
- NIDCR grants DE011111, DE017921, DE012505, DE016690 and DE023193
- Lamont lab members

Characterization of acidic pH functionalized mesoporous silica nanoparticles for ovarian cancer diagnostics

Benjamin Fouts, Phillip Chuong, Lacey R. McNally

Department of Medicine, University of Louisville, Louisville, KY

ABSTRACT

Purpose: Current FDA approved clinical screening approaches for ovarian cancer, such as CA-125 and TVU, have been shown in recent years to provide minimal improvements to overall survival rates. This is due to the majority of ovarian cancer diagnoses coming at later stages of the disease, which leads to poor survival that could be avoided if better early detection were available. More effective screening agents are therefore necessary for improving diagnostic imaging of ovarian cancer. | Diagnostic studies using larger MSNs (50-200nm) have been successful at targeting tumors *in vivo*, although an optimal particle size range of 15-50nm has been identified for avoiding RES screening and rapid excretion. Mesoporous Silica Nanoparticles (MSNs) of this medium size range have relatively low blood clearance compared to smaller or larger particles, and have far lesser lytic impact on erythrocytes (RBCs), serum material, cellular uptake viability, and vital organ function than their non-porous counterparts and other nanomaterials such as iron oxide, gold and silver. Mesoporous silica was therefore chosen as a core particle in this study, with size variation as a key variable to be investigated. | In conjunction with choice of nanomaterial, selection of a tumor targeting agent also determines particle efficacy in diagnostic imaging. Few biomarkers that have high expression fidelity over all variants of ovarian cancer are useful for targeting with high accuracy. This study therefore utilizes novel pH Low Insertion Peptide Variant 7 (V7 pHLIPs or pFLIPs) for its dual pH –specific activity, being inert at physiologic pH and possessing active transmembrane insertion properties at weakly acidic pH. We hypothesize that the merger of V7 targeting and a mesoporous silica nanomaterial platform will improve particle targeting for its size.

Methods: We utilized a modified Stober method to generate small, mesoporous silica nanoparticles (MSNs) based upon Tetra(methyl/propyl) Orthosilicate (Scheme 1). Following dialysis in acetic acid and ammonium nitrate (AN), the core MSNs were then conjugated with (3-aminopropyl) triethoxysilane (APTES) and (3-Glycidyloxypropyl) trimethoxysilane (GPTMS), subsequently being coated with a chitosan polymer solution. At low pH, IR-780 dye was introduced and encapsulated. The MSN core further conjugated with 4-(*N*-Maleimidomethyl) cyclohexanecarboxylic acid *N*-hydroxysuccinimide ester (SMCC) and V7 pHLIP to produce a sensitively pH targeted, dye release agent (CVM-Me) for further *in vitro* and *in vivo* study. *In vitro* studies were performed with 6 well plates of ES-2 and A2780 cell lines grown in RPMI media. Particles were also evaluated in tissue phantoms by the method of Multispectral Optoacoustic Tomography (MSOT). Subsequently, CVM-Me particles containing IR-780 dye were iv injected into mice bearing ES-2 tumors with bio-luminescence being determined by Advanced Molecular Imaging (AMI) and particle distribution determined by MSOT.

Results: CVM-Me's size, 25.52 nm (average of 22 particles), as well as mesoporosity, was shown via Transmission Electron Microscope (TEM) images (Figure 1); this was corraborated by DLS measurements (Figure 2). DLS studies (Figure 3) showed size of core M-Me at 2h was not significant from that at 18h ($p<0.05$); the size difference between P-Pr at 2h and 18h however was significant ($p=0.17$). M-Me growth may therefore be static over the 18h period reported in its original synthesis procedure, whereas P-Pr is seen to grow continuously over the 18h period. | Washing repeatedly in MQ water following acetic acid dialysis yielded apparent decreases in d.n.m as measured by DLS (Figure 4). The trend for both core particles was rapid decrease in d.n.m from 2-6 washes followed by a 10-fold slower decrease from 6-21 washes. This indicates that major extraction of acid and/or CTAB may have occured most prominately during early during washing. | ζ-Potential measurements confirmed chitosan coating by differentiated response to varying pH microenviroments (Figure 5). With AN absent from the chitosan coated (CC) particle cores, a significant increase in zeta potential is observed between pH 7.4 and pH 6.6 for M-Me 18h ($p<0.0001$), M-Me 2h ($p=0.0016$), P-Pr 2h ($p<0.0001$), ANM-Me 18h ($P<0.0001$), and ANM-Me 2h ($p<0.0001$). For P-Pr 18h ($p=0.1788$), ANP-Pr 18h ($p=0.2995$), and ANP-Pr 2h ($p=0.5747$) the effect of varied protonation of chitosan at pH 7.4 and pH 6.6 was not significant. That all M-Me samples showed pH responsiveness in ζ-Potential measurements suggests that the particles' size may lend itself better to shifts in charge than the larger P-Pr particles. | *In vitro* studies in Odyssey (Figure 6) and MSOT (Figure 7) showed preferential particle uptake of CVM-Me in ES-2 and A2780 ovarian cancer cells at pH 6.6. This suggests proper activation of the V7 ligand. | *In Vivo* studies in laboratory mice (Figure 8) found that CVM-Me showed higher uptake in orthotopic ovarian cancer tumors than in the liver, spleen, or blood, at 4h post-injection.

Conclusion: We found that length of time during synthesis at 80°C increased particle size minimally for M-Me, though not for P-Pr. Various characterizations showed that M-Me may be more suitable to shortened synthesis and effective dye release over the larger P-Pr. Dual acidic pH targeting, using both chitosan and V7 peptide, CVM-Me's tumor specificity. CVM-Me demonstrated tumor specificity in vivo as detected using MSOT.

Synthesis Schematic of CVM-Me

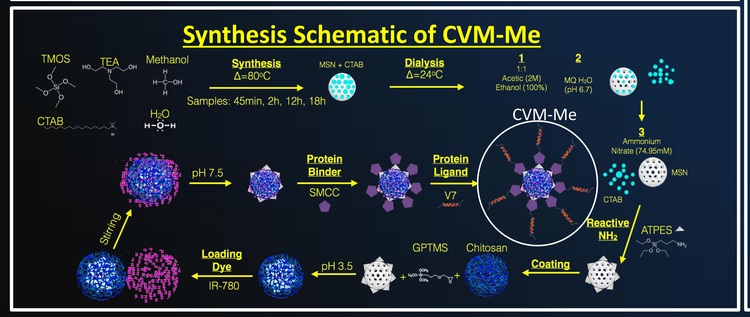

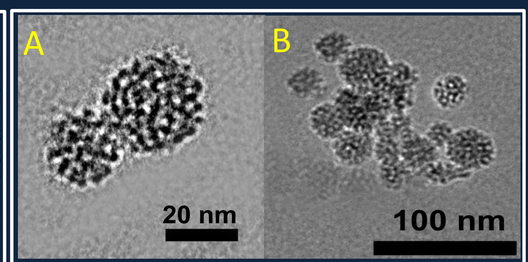

Figure 1: Transmission Electron Microscope (TEM) images of core MSNs. An average particle size of 25.58 +- 3.1nm was calculated by measuring 22 particles on Image J software.

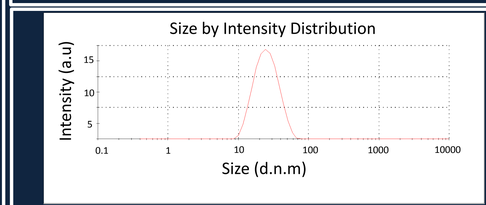

Figure 2: DLS size measurement of core M-Me particle at a synthesis time of 1h. Average size at t = 1h is 26.44 d.n.m.

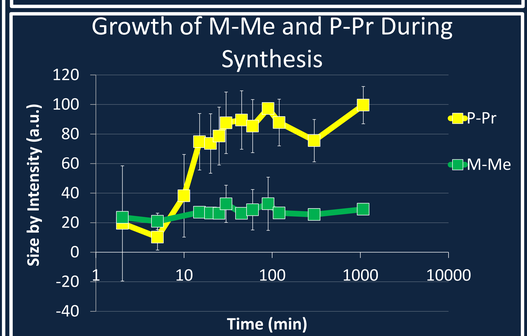

Figure 3: Dynamic Light Scattering (DLS) measurements of the MSN core during synthesis from TMOS, TEA, CTAB, and Methanol at 80°C. Measurements for both M-Me and P-Pr were taken at various times between 2 minutes and 18h. The measure of time on the x axis in minutes is on a logarithmic scale. Intensity measurements are shown in arbitrary units. Error bars represent standard deviation (some are hidden under points due to small size). M-Me size at 2h was not statistically different from that at 18h ($p<0.05$), though size increase for P-Pr over the size time period was significant ($p=0.17$).

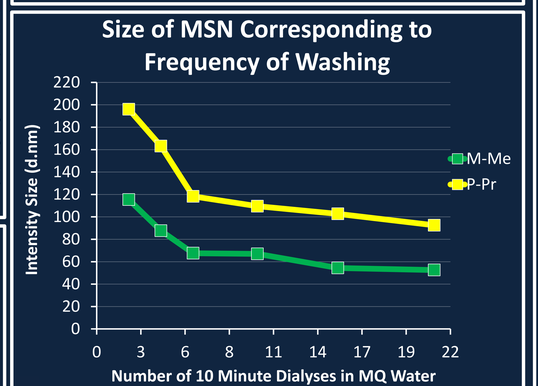

Figure 4: A comparative study of the decrease in size of MSNs synthesized by the mechanism outlined in the synthesis schematic, though with M-Me synthesized from TMOS and methanol and P-Pr synthesized from TPOS and propanol. The trends from 2-6 washes were -19.425 d.n.m/wash and -11.96 d.n.m/wash for P-Pr and M-Me respectively. Washes 6-21 had a 10-fold reduced impact on size.

RESULTS

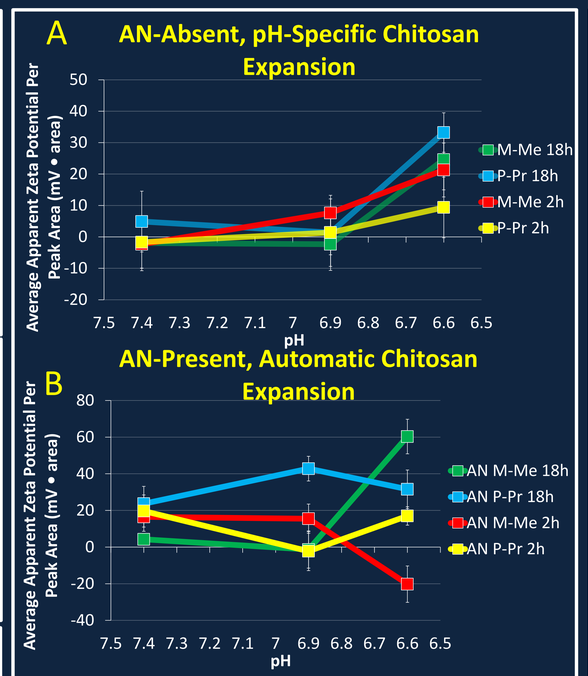

Figure 5: (AN-absent) MSNs without post-synthesis ammonium nitrate washing, M-Me 18h, P-Pr 18h, M-Me 2h, and P-Pr 2h. all showed a pH specific response during ζ-potential measurement following overcoating of particle cores with chitosan; (AN-Present) MSNs with post-synthesis ammonium nitrate washing, AN M-Me 18h, AN P-Pr 18h, AN M-Me 2h, and AN P-Pr 2h, appear to exhibit constant expansion of an applied chitosan overcoating during zeta potential measurements. This is only consistently significant for M-Me particles. Error bars represent the standard deviation.

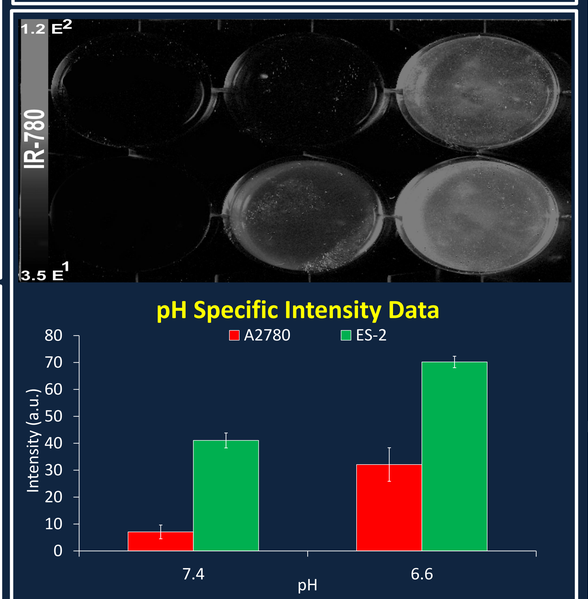

Figure 6: Evaluation of CVM-Me particle binding specificity in the context of acidic pH. A2780 and ES-2 cell lines in pH-specific media (7.4 and 6.6). Cell lines were plated in 6-well plates in pH-non-specific media for growth, and growth media was changed to pH 7.4 (top) and 6.6 (bottom) to simulate the difference in pH of normal body tissue (pH 7.2-7.4) and tumorous tissue (pH 6.6-6.8). Final particle concentration in the wells was calculated based on the optimal V7 (pHLIP) concentration. CC-MSN-V7 showed 4.52x signal at pH 6.6 over pH 7.4 in A2780 cells, whereas it showed 1.70x signal at pH 6.6 over pH 7.4 in ES-2 cells. Error bars represent standard deviation.

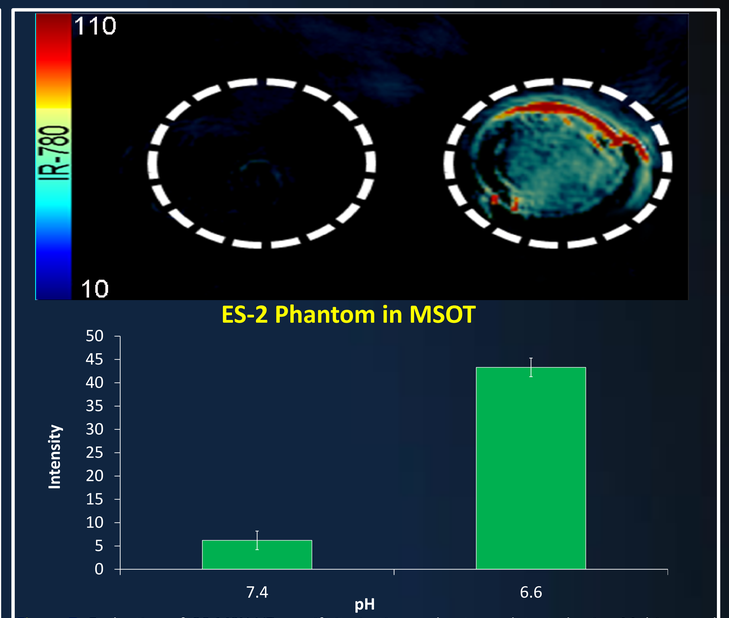

Figure 7: Evaluation of CC-MSN-V7 specificity in tissue phantoms detected using Multispectral Optoacoustic Tomography (MSOT). Cells were taken from a six well plate where they were grown in non-pH specific media, and then transferred to 7.4 and 6.6 pH media, respectively, before incubation with CC-MSN-V7. CC-MSN-V7 showed 6.98x signal in pH 6.6 over pH 7.4 in the gel phantoms, as compared to 1.70x in the above Odyssey plate. Error bars represent standard deviation

CVM-Me Biodistribution Imaging *in vivo* by MSOT

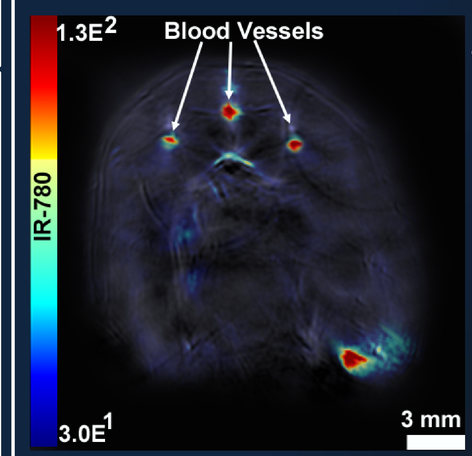

Figure 8: Multispectral optoacoustic tomography detects tumor accumulation of CVM-ME 4h post injection. Athymic mice bearing subcutaneous ES-2 tumors were injected with 2.8 mg nanoparticles/ 100 µl PBS. Specific particle accumulation in the tumor was observed, with minimal uptake in the liver, kidneys, and spleen.

Conclusions

- We synthesized an MSN of 25.58 ± 3.1nm
- Increasing MSN core synthesis time increased size minimally for M-Me core particles, though not for P-Pr.
- Z-Potential measurements indicate the smaller M-Me platform may be more versatile for chitosan attachment.
- CVM-Me demonstrated acidic pH specificity as observed using NIR fluorescent imaging *in vitro*.
- CVM-Me specifically accumulated within the ovarian tumor 4h post iv injection as identified using multispectral optoacoustic tomography.

Acknowledgements

We would like to thank the NCI for generously funding the R25 Program, and this research, through the R25-CA134283 grant. We especially appreciate the support of the James Graham Brown Cancer Center and the University of Louisville School of Medicine. Further, we are thankful for the efforts of Molly McNally throughout this experimentation.

Investigation of CRISPR/Cas9 Arylamine N-Acetyltransferase 1 Knockout MDA-MB-231 Cell Lines via Anoikis and Invasion Assays

Madison M. Furnish, Marcus W. Stepp, Mark A. Doll, Maggie Y. Chang, and David W. Hein

Department of Pharmacology and Toxicology and James Graham Brown Cancer Center
University of Louisville, School of Medicine, Louisville, KY

Abstract

Arylamine N-acetyltransferase 1 (NAT1) was originally discovered as a xenobiotic metabolizing enzyme. NAT1 is ubiquitously expressed in human tissue. The endogenous role of NAT1 in breast cancer piqued our interest due to high levels of expression of NAT1 in ER positive breast cancers. We investigated the MDA-MB-231 cell line, which has relatively lower NAT1 expression than its ER positive counterparts. MDA-MB-231 CRISPR/Cas9-mediated knockouts have been created with no detectable NAT1 activity. These cell lines showed a dramatic difference in the ability to form colonies in soft agar, which suggests that the absence of NAT1 affects anchorage-independent growth. Therefore we utilized the MDA-MB-231 CRISPR/Cas9 NAT1 knockouts in this investigation to test anchorage-independent growth and invasive abilities. We hypothesized that the knockouts would be susceptible to anchorage-dependent apoptosis (anoikis) and have a decreased invasive ability compared to the parental line. Both the CRISPR/Cas9-mediated NAT1 knockout and the parental line were compared side by side in anoikis assays spanning six days, Transwell® invasion, and migration assays. Albeit prior literature reported a decrease in invasive ability *in vitro*, we determined that the absence of NAT1 in MDA-MB-231 cell lines had little to no effect on anchorage-independent growth and the cellular invasion ability (P= 0.19). Thus, the absence of NAT1 in MDA-MB-231 cells did not affect anchorage-independence or invasion, but rather the ability of those cells to grow in close proximity to one another.

Hypothesis

As supported by previous literature, we hypothesize that the CRISPR/Cas9-mediated NAT1 knockouts will have a decreased invasive ability in MDA-MB-231 cell lines compared to the parental line. The dramatic differences in soft agar colony formation led us to hypothesize that the CRISPR-Cas9-mediated knockouts may have a decreased ability for anchorage-independent growth.

Methods

CRISPR/Cas9 Constructed NAT1 Knockout
MDA-MB-231 parental cell lines were transiently transfected with a single plasmid containing GFP, Cas9, and either guide RNA 2 or 5. Cells were sorted/collected for GFP expression and allowed to grow into single-cell colonies. Initial characterization was done with RFLP-PCR.

Anoikis Assay
- 96 well plates were coated with two layers of poly-HEMA. The poly-HEMA was made by diluting 50 mg/ml stock at a 1:10 ratio in 100% ethanol for a final concentration of 5.0 mg/ml. Plates were dried over night between each coating.
- 4.0 x 10^3 cells in 100 µL of complete media including a 0 cell control was added for each condition. Cells were incubated over night before recording the 0 hour reading. Before reading, 10 µL of AlmarBlue® was added to each well and incubated for 3 hours. A reading was taken from 0 to 120 hours every 24 hours.

Invasion Assay
- **A.** 100 µL of Matrigel® was added at the bottom of 24 well Corning®Transwell® inserts and cured for 2 hours at 37°C with 5% CO_2.
- **B-C.** Inserts were seeded with 5.0 x 10^4 or 2.5 x 10^4 cells resuspended in minimal media. Complete media was used as a chemoattractant and added at the bottom, separate from the Matrigel®-filled insert. The inserts incubated at 37°C with 5% CO_2 for 24 hours.
- **D.** To visualize the cells, we fixed the cells with 10% formalin, dyed them for an hour in crystal violet, and washed with water 3 times.

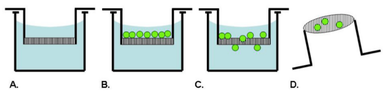

(Illustration)) Hulkower & Herber, *Pharmaceutics* **2011**, *3*, 107-124

Results

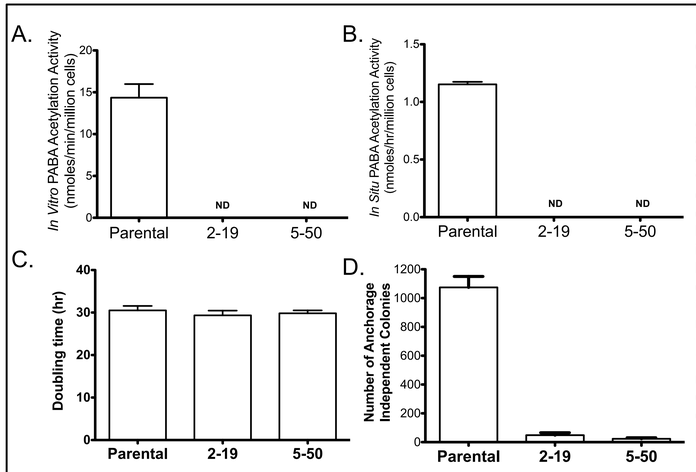

Figure 1 – Characterization graphs of MDA-MB-231 parental and CRISPR/Cas9 NAT1 knockout cell lines. A) The *in vitro* NAT1 enzymatic activity. **B)** The *in situ* NAT1 activity of the cells. There was no detectable activity in either measure of activity (**A** or **B**) for the knockout cell lines. **C)** The doubling time in hours for the three cell lines. There was no difference between the three cell lines. **D)** The number of colonies able to form in a soft agar assay. There was a significant reduction of soft agar colonies for the CRISPR cell lines compared to the parental line.

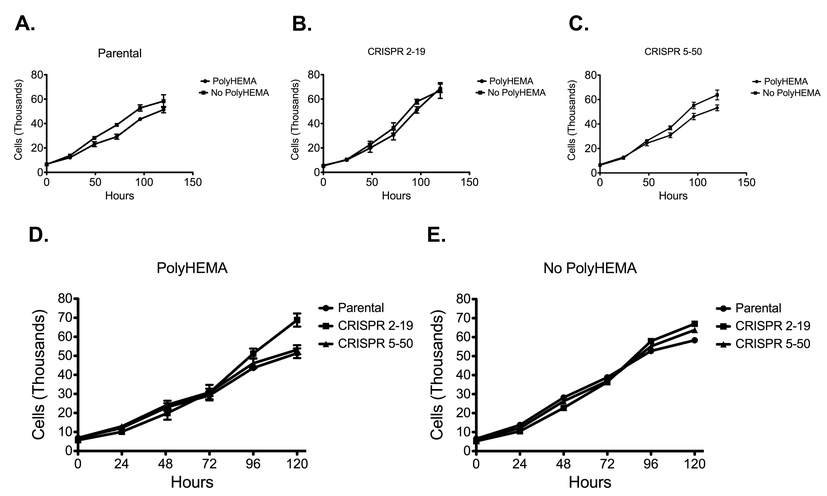

Figure 2. – Growth curves for MDA-MB-231 cell lines with standard adhesion or anchorage-independent conditions. A-C) Parental and CRISPR cell lines growth curves comparing its ability to grow in poly-HEMA coated wells (anchorage-independent conditions) versus standard non-coated wells. Parental and the CRISPR/Cas9-mediated NAT1 knockouts displayed a high level of anoikis resistance when compared to standard anchorage growth. Comparisons of the two different conditions for each cell line by Student's T-test showed no statistical difference (A. p=0.63; N=3 / B. p =0.88; N=3 / C, p=0.72; N=3). **D-E)** Contrary to the hypothesis, the NAT1 knockouts had comparable anoikis resistance to the parental strain. Each cell line was grown in poly-HEMA coated wells or standard wells over the course of 6 days. Comparison of these resulting curves showed strong similarity between each cell line.

Results

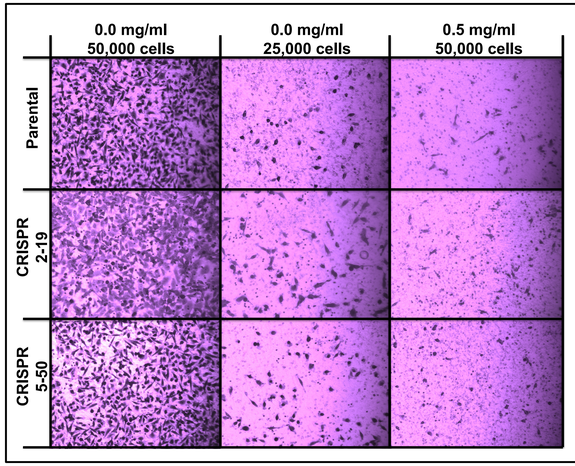

Figure 3 – Comparison of photomicrographs taken of the bottom side of Transwell® insert membranes. This figure illustrates the different number of cells that were able to reach the bottom side of the membrane either with or without gel for parental or CRISPR NAT1 knockout cell lines. The gel concentration is given along the top of the columns as mg/ml, and then directly below is the number of cells that were seeded into the Transwell® insert.

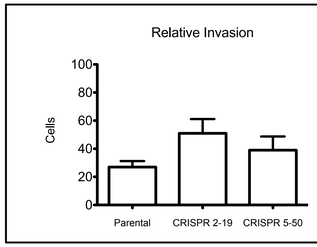

Figure 4 – Relative Invasion ability for MDA-MB-231 parental and NAT1 knockout cell lines.

Relative invasiveness was calculated by dividing the cells that invaded through the 0.5 mg/ml gel matrix (insert seeded with 50,000 cells) by the number of cells that migrated through no gel (insert seeded with 25,000 cells). The resulting one-way ANOVA of the relative invasiveness value for each cell line was non-significant (P=0.19; N= 4).

Conclusions

We examined anoikis resistance and invasive ability of NAT1 knockouts in MDA-MB-231 breast cancer cell lines. Previous data from our lab showed the CRISPR/Cas9-mediated NAT1 knockouts yielded significantly fewer colonies in soft agar assays. To further understand what may be causing the difference soft agar assays, we investigated the CRISPR/Cas9 knockouts anoikis resistance in comparison to their parental lines. The data showed that NAT1 knockout cell lines retained the same level of anoikis resistance as the parental cell line. In this study we also investigated NAT1 knockout cell lines ability to invade through the Transwell® membrane. The results suggest that there was no significant difference between parental and NAT1 knockout cell lines. Further studies may examine the mechanism by which MDA-MB-231 NAT1 knockouts appear to be inhibiting their own growth in close proximity. Understanding NAT1s role in breast cancer may lead to a novel approach in inhibiting cellular metastasis.

Acknowledgements

Research funding was supported by the University of Louisville and the National Cancer Institute R25-CA134283 grant.

A special thanks to the Hein lab and members from States, Kidd, Siskind, and Beverly labs.

Functional Interaction Between NORE1A and Mutationally Activated RIT(Q79) Represses Malignant Transformation in Lung Cancer

Ashley M. Gleaton[1], M. Lee Schmidt, Ph.D. [1,2], and Geoffrey J. Clark, Ph.D.[1,2]

[1] Molecular Targets Group, James Graham Brown Cancer Center and [2] Department of Pharmacology & Toxicology
School of Medicine, University of Louisville, Louisville, KY, USA

INTRODUCTION

Mutationally activated RIT (*RIT1*-Q79L), a Ras-related GTP-binding oncoprotein, was not considered important in carcinogenesis until recently. RIT is now identified as a key oncogenic mutation in about 3% of lung cancer cases, determined by the mass genomic sequencing of tumors. Lung cancer is the most common cause of cancer death in the United States for both men and women. Every year, this translates to more than 5,000 people being diagnosed with incurable RIT-driven lung cancer. Yet, for the process by which mutationally activated RIT contributes to lung cancer as well as the signal transduction pathways involved remain largely unknown. We have identified the tumor suppressor NORE1A as a novel direct binding partner of RIT in a yeast two hybrid screen. Here we show that NORE1A and RIT can complex in mammalian cells and that NORE1A acts as a protection mechanism against RIT-mediated hyper-stimulation of growth and development pathways. Suppression of NORE1A expression was essential for RIT to express its transforming phenotype. In tumor cells, NORE1A is often silenced by epigenetic inactivation hence, knockdown of its expression will facilitate tumor formation due to RIT. The importance of identifying and characterizing this interaction, as well as understanding its mechanism of action in the event of lung carcinoma may lead to the development of better targeted therapies for RIT driven lung cancer.

METHODS

Cell Lines: NIH 3T3 cells are a mouse fibroblast cell line and were maintained in DMEM with 10% calf serum (CS) and 1% penicillin-streptomycin and HEK293 cells in DMEM with 10% fetal bovine serum (FBS) and 1% penicillin-streptomycin. NIH 3T3-shSCRAM is stably transfected with a scrambled control shRNA. NIH 3T3-shNORE1A 367 and NIH 3T3-shNORE1A 971 were knocked down for NORE1A expression. All three cell lines- NIH 3T3-shSCRAM, NIH 3T3-shNORE1A 367, NIH 3T3-shNORE1A 971- were constructed and generously gifted by Dr. Howard Donninger.

Luciferase Assays: HEK293 cells are human epithelial cells that were transfected with expression constructs tagged with fluorescent protein (GFP) or human influenza hemagglutinin (HA), incubated for 24 hours and then lysed. NIH 3T3 cells were transfected with expression constructs tagged with fluorescent protein (GFP), incubated for 24 hours and then lysed. Gene expression in HEK293 and NIH 3T3 cells was measured using a Dual Luciferase Kit from Promega along with a Berthold Technologies Lumat LB 9507 tube luminometer.

Proliferation Assays: NIH 3T3 cells were seeded in the wells of a 6 well plate. Each cell line was transfected with expression constructs tagged with fluorescent protein (GFP) and incubated at 37°C. Cell counts were taken every 24 hours using a hemocytometer.

Soft Agar Colony Formation Assays: NIH 3T3 cells were transfected with expression constructs tagged with fluorescent protein (GFP), suspended in 0.35% agar solution and seeded on 0.7% agar base in the wells of a 6 well plate. The cells were incubated at 37°C for two weeks before colony counts were measured.

RESULTS

1

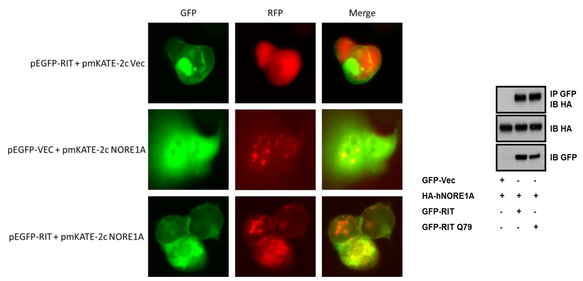

Figure 1: NORE1A interacts with the small-GTPase RIT. NORE1A and RIT were initially identified as binding partners by a yeast two-hybrid screen. We sought to confirm this result by using two different assays. First, fluorescence microscopy images of GFP-RIT paired with a RFP (KATE) tagged NORE1A shows that these two proteins co-localize on both the cellular membrane as well as in punctate structures in the nucleus. Next we used a co-immunoprecipitation assay where cells, transfected with GFP-tagged wild-type RIT and mutationally activated RIT, were immunoprecipitated using GFP-agarose beads. Here we found that NORE1A binds strongly to both wild-type and mutationally activated RIT.

2

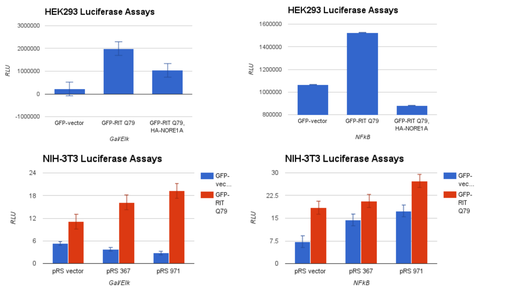

Figure 2: NORE1A suppresses RIT mitogenic signaling. HEK293 cells were transfected with GFP-vector, GFP-tagged RIT Q79 or GFP-tagged RIT Q79 and HA-tagged NORE1A. When RIT is mutationally activated, large increases are observed in both Gal/Elk ($p<0.05$) and NFκB transcriptional activity. When NORE1A is co-expressed with activated RIT, Gal/Elk and NFκB activation are suppressed in HEK293 cells. NIH-3T3 cells were transfected with GFP-vector (blue) or GFP-tagged RIT Q79 (red) in combination with previously validated shRNA constructs for NORE1A including a scrambled vector control and two different shNORE1A sequences. Suppression of NORE1A allows activated RIT to more powerfully activate Gal/Elk transcriptional activity ($p<0.05$) supporting our results from the HEK293 cells. In regards to NFκB activity in NIH-3T3 cells with mutationally activated RIT, we did not observe NORE1A following a similar trend.

3

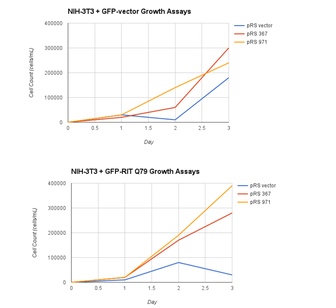

Figure 3: NORE1A suppresses RIT mediated growth stimulation in NIH-3T3 cells. NIH-3T3 cells were transfected with GFP-vector or GFP-tagged RIT Q79 into stable cells lines expressing a scrambled shRNA vector control along with two shRNA constructions against NORE1A. Activated RIT was only able to enhance cell growth in the absence of NORE1A expression supporting our hypothesis that NORE1A likely functions as a cellular protection mechanism against mutational activated RIT growth stimulation.

4

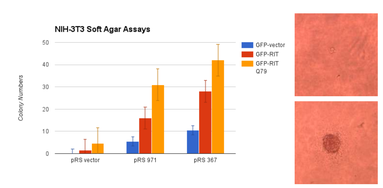

Figure 4: Loss of NORE1A expression increases tumorigenic potential of NIH-3T3 cells in the presence of activated RIT. Three NIH 3T3 cell lines- shSCRAM, shNORE1A 367, shNORE1A 971- were transfected with GFP-vector (blue), GFP-tagged RIT (red) or GFP-tagged RIT Q79 (yellow) in the presence (pRS vector) or absence (pRS 367, 971) of NORE1A expression. The top right image is a representative single-cell of NIH-3T3 in agar while the bottom right image is a representative tumor colony of NIH-3T3 observed. Our results show that the loss of NORE1A expression significantly increased anchorage-independent growth in NIH 3T3 cells with either wild-type RIT or mutationally activated RIT ($p<0.05$) suggesting that RIT can drive transformation either by increased stoichiometry or mutational activation.

5

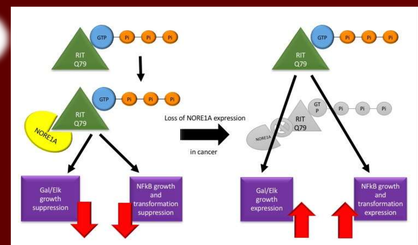

Figure 5: Schematic of proposed RIT Q79/NORE1A tumor suppressor pathway. NORE1A binds and suppresses mutationally activated RIT (Q79) oncoprotein directly, resulting in the suppression of RIT growth and transformation signaling via Gal/Elk pathway regulation and NFkB growth and transformation signaling control. In human cancers, loss of NORE1A expression prohibits this functional interaction, leading to excessive proliferation signaling through a number of pathways including Gal/Elk and NFkB signaling mechanisms.

DISCUSSION

RIT has been now identified as a driving mutation in about 3% of lung cancer cases, although the signal transduction process by which mutationally activated RIT may contribute to cancer remains unknown. We have identified a tumor suppressor called NORE1A as a direct binding partner of RIT. Studies in which we examined the action of RIT in cells knocked-down for NORE1A showed that NORE1A suppresses both the mitogenic signaling and the transforming activity of RIT. As NORE1A is frequently inactivated by promoter methylation in lung tumors, NORE1A inactivation may be essential for the development of RIT driven lung cancer.

Conclusions

1. NORE1A and RIT form a complex in mammalian cells.
2. NORE1A suppresses the mitogenic and tumorigenic phenotype of RIT oncogenes.
3. Epigenetic therapy to restore NORE1A expression may be a novel approach to suppress RIT-driven lung cancer.

ACKNOWLEDGEMENTS

Research was supported by the NCI R25 grant University of Louisville Cancer Education Program NIH/NCI (R25-CA134283). Special thanks to the Dr. Lee Schmidt and Clark lab for their assistance with this project.

Tamoxifen: A Study in Pharmacovigilance

Zahara Gully, Candidate BS Exercise Science; Demetra Antimisiaris, PharmD..
Departments of Pharmacology and Toxicology, University of Louisville School of Medicine

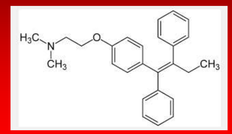

UNIVERSITY OF LOUISVILLE
It's Happening Here.

Background

Chronic medication use in chronic diseases along with chronic cancer treatment could lead to further medical conditions as a result of inadequate monitoring. The percent of older adults is growing and as such, the percent of persons living with breast cancer as a chronic disease is growing .(1)One medication which is a corner stone of long term breast cancer therapy is Tamoxifen.

The traditional course of treatment spans approximately 5 years, and since the findings of the ATLAS study in 2015, the standard of care will increase the average length of Tamoxifen treatment to 10 years . (2)

Adverse drug events account for a high percentage of hospitalizations in older adults and estimates reveal that up to 33% of all hospitalizations in older adults are due to medication related problems (3)One means of preventing adverse drug events is through adequate monitoring and pharmacovigilance. (4,5)

The medical literature describes the common adverse events which with tamoxifen is associated. (6) Namely, hypercalcemia (especially with initiation of therapy and in patients with bone metastasis), deep vein thrombosis (DVT), pulmonary embolism (PE), stroke, and uterine malignancies.

Appropriate pharmacovigilance for chronic Tamoxifen use also includes: tolerability, duration of therapy, drug interactions, and drug disease interactions (contraindications).

Objective

To characterize and discuss the current state of Tamoxifen pharmacovigilance in a sampling of a patient population.

Hypothesis

We hypothesize that individuals being administered Tamoxifen are not being appropriately monitored which could lead them to increased risk of medical conditions arising such as hypercalcemia, uterine malignancies, or stroke.

Methods

We requested identification of patients who are currently taking tamoxifen regardless of age, or practice, from all of the outpatient clinics within our healthcare system. The confidential and HIPPA protected data provided by our health system IT data specialist yielded 93 patients receiving tamoxifen therapy. A patient identification key was created, numbering each patient sequentially and the key kept separately and securely from the patient identification list.
The data collected includes documentation in the electronic health record of: indication for tamoxifen use, drug allergies, tamoxifen dose, duration of tamoxifen therapy, presence of calcium supplementation, concurrent use of bone density medications, presence and date of calcium level monitoring, PTH level, documentation of deep vein thrombosis, pulmonary emboli or stroke monitoring, presence of a history of hypercoagulability (DVT, PE, or stroke), bone metastasis, monitoring for uterine malignancies, history of uterine malignancies, warfarin or anticoagulation use. Our data focuses on the presence or lack of documentation regarding safe tamoxifen use.

Results

Data Collected		
Number of Charts/Subjects	93	
Age Range of Subjects	60-100	
Average Age of Tamoxifen User	70.5	
Missing Indication for Tamoxifen Use	6	6.4%
Duration of Therapy Documentation (ATLAS study:10 yrs.)	All documented	One two years over 10 yrs.
Calcium Monitoring Absent	26	28%
No Calcium Level Documented Within Past Year of Levels on Record.	43/67	56.5% not current One notation for Ca++ monitoring monthly for first year, then bi-annually the next year, then annually thereafter. (appropriate Ca++ monitoring with Tamoxifen use)
Absent documentation of screen for DVT, PE or Stroke (Increased clot risk with Tamoxifen use.)	90/93	96.7% Positive Documentation: Case 1: "no sign/symptoms of DVT" Case 2: "no s/s of stroke or MI" Case 3: "no s/s of DVT"
Patients receiving Tamoxifen therapy with a history of stroke, DVT, or PE	2	2.1% Not the same cases as above.
Absent documentation of monitoring for uterine malignancies.	90/93	96.7% absent Positive Documentation: Cases 1-3: "Reminder to check bone density, cervical pap smear, and mammogram."
Patients receiving Tamoxifen therapy with the presence of a history of uterine malignancy.	1	This case was not one of the 3 cases listed positive for uterine malignancies monitoring documented or in the care plan.
Patients receiving concurrent Warfarin or other Anticoagulant therapy. (Tamoxifen is pro-thrombic)	2	One case taking Warfarin and one taking dabigatran

Contraindications for Tamoxifen: Known hypersensitivity to the drug or any of its ingredients; in women who require concomitant coumarin-type anticoagulant therapy or in women with a history of deep vein thrombosis (DVT) or PE (reduction of breast cancer incidence in high-risk women/DCIS only).

Tamoxifen citrate [package insert]. Corona, CA: Watson Laboratories; July 2011.

Boxed Warning

Ductal carcinoma in situ/women at high risk for breast cancer:

Serious and life-threatening events associated with tamoxifen in the risk-reduction setting (women at high risk for cancer and women with ductal carcinoma in situ [DCIS]) include uterine malignancies, stroke, and pulmonary embolism (PE). Incidence rates for these events were estimated from the National Surgical Adjuvant Breast and Bowel Project (NSABP) P-1 trial. Uterine malignancies consist of endometrial adenocarcinoma (incidence rate per 1,000 women-years of 2.2 for tamoxifen versus 0.71 for placebo) and uterine sarcoma (incidence rate per 1,000 women-years of 0.17 for tamoxifen versus 0.4 for placebo) (updated long-term follow-up data [median length of follow-up is 6.9 years] from NSABP P-1 study). For stroke, the incidence rate per 1,000 women-years was 1.43 for tamoxifen versus 1 for placebo. For PE, the incidence rate per 1,000 women-years was 0.75 for tamoxifen versus 0.25 for placebo.

Some of the strokes, PE, and uterine malignancies were fatal. Discuss the potential benefits versus the potential risks of these serious events with women at high risk of breast cancer and women with DCIS considering tamoxifen to reduce their risks of developing breast cancer. The benefits of tamoxifen outweigh its risks in women already diagnosed with breast cancer.[1]

Tamoxifen Black Box Warning: Source, Drug Facts and Comparisons

Discussion

We hypothesized that individuals being administered Tamoxifen are not being appropriately monitored which could lead them to increased risk of medical conditions arising such as hypercalcemia, uterine malignancies, or stroke. Our results reveals consistent gaps in monitoring, despite the rare case of attempts to provide appropriate monitoring.

As the clinical adage goes: "if it is not documented, it didn't happen". A significant source of lack of documentation appears to be incomplete records. For example, a patient seen by our system for reconstructive surgery, where the sole documentations are the medications and surgery procedure summary note for clinic follow up, devoid of any laboratory findings or progress notes. This gap in documentation causes a missed opportunity for each clinician who accesses the patient chart to have the data at hand to perform pharmacovigilance and drug use surveillance. Most serious adverse drug events are not discovered until the case enters the ER door, and 1 in 3 hospital admissions in older adults are due to adverse drug events, yet, appropriate drug use monitoring is one means to prevent unnecessary medication related harm. (7,8)

The average office visit consists of 15 minutes, of which 7 are used for establishment of the topic or problem to work on, leaving 3.5 for problem solving and 3.5 for medication management. (9) Thus, it is easy to understand why patient records are incomplete. The mandate to use EHRs by the affordable care act was a step towards the possibility of universal health records, which may some day help improve the problem of incomplete charts.

Conclusions

This study provides a description of the current status of Tamoxifen Pharmacovigilance and can be a starting place for benchmarking improvements in Tamoxifen safety and use quality improvement interventions.

Acknowledgments

National cancer Institute R25 research Grant and the James Brown Cancer Center Summer Research Program

References

1. Risk Factors Associated with Loco-Regional Failure after Surgical Resection in Patients with Resectable Pancreatic Cancer. Hyun Ju HJ Kim PLoS ONE 11(6) Public Library of Science 2016 1932-6203
2. Long-term effects of continuing adjuvant tamoxifen to 10 years versus stopping at 5 years after diagnosis of oestrogen receptor-positive breast cancer: ATLAS, a randomised trial. Christina C Davies Lancet, The 381(9869) Elsevier 2013-3-9 0140-6736
3. The impact of a Medication Review with Follow-up service on hospital admissions in aged polypharmacy patients. A A Malet-Larrea British Journal of Clinical Pharmacology Wiley 2016-5-14 0306-5251
4. **Budnitz DS, Lovegrove MC, Shehab N, et al**. Emergency Hospitalizations for Adverse Drug Events in Older Americans. NEJM 365;21: 2002-2012 Nov 24 2011.
5. **Gurwitz, JH., Field TS., Harrold LR., et al**. Incidence and Preventability of Adverse Drug Events Among Older Persons in the Ambulatory Setting. JAMA March 5, 2003 Vol 2389, no 9 1107-1116
6. Nolvadex FDA drug monograph. http://www.accessdata.fda.gov/drugsatfda_docs/label/2005/17970s053lbl.pdf (accessed June 23,2016)
7. Budnitz DS, Lovegrove MC, Shehab N, et al. Emergency Hospitalizations for Adverse Drug Events in Older Americans. NEJM 365;21: 2002-2012 Nov 24 2011
8. Page RL II, Ruscin JM. The risk of adverse drug events and hospital-related morbidity and mortality among older adults with potentially inappropriate medication use. *Am J Geriatr Pharmacother*. 2006;4(4):297–305.
9. Tai-Seale, M., McGuire, T. G., & Zhang, W. (2007). Time allocation in primary care office visits. *Health Services Research*, *42*(5), 1871–1894.